## Results and Discussion

Calculations were carried out on some of the important spacer materials, namely Dexiglas (C. H. Dexter and Sons Paper Co.), Tissuglas (Pallflex Products Co.), silica fiber felt (called "refrasil," H. I. Thompson Co.)[6] and low-density foam (freon blown polyurethane with density $\approx 2$ lbm/ft$^3$).[7] No reliable data for the extinction coefficient of these materials are available. The values used here are from Cunnington et al. for a source temperature of 500°K with an estimated experimental error of 50%. The results presented in Table 1 indicate that the correction on the extinction coefficient is negligible for these materials under normal values of spacer thickness and shield reflectance. This implies that the influence of wall reflections on the heat transfer is small compared to that due to spacer scattering.

It is also clear from Table 1 that the extinction coefficients of most of the spacer materials are large enough that the optically thick situation exists. The effective conductivity $\kappa_e$ is given by

$$\kappa_e = \kappa + \kappa N(1 + \theta_2)(1 + \theta_2^2) \qquad (7)$$

where $\theta_2 \equiv T_2/T_1$. The first term on the right-hand side is the conduction contribution, while the second term represents the radiation contribution.

These calculations also reveal that under normal working conditions, radiation plays an insignificant role in the lateral heat transfer when Dexiglas or Tissuglas is used as spacers. The scattering is so large in these cases that it effectively localizes the radiation. These observations are borne out by the fact that theoretical predictions of Tien et al.[8] on the basis of purely conductive heat transfer with size effect agree well with the data of Coston and Vliet.[3] In the case of silica fiber felt or low-density foam spacer systems, substantial contribution to the lateral heat transfer from radiation is expected. However, there are no data available to check the validity of these predictions. It should be emphasized here that the above calculations are based on the assumption that the gap spacing is completed filled with the space material. For loosely packed spacers as in most applications a greater contribution of radiation than predicated is expected.[10]

Pogson and MacGregor[11] have analyzed the problem of selective slitting of individual layers to increase the thermal resistance due to conduction. This will have an effect of increasing the percentage of radiative contribution to the total heat transfer; however, the two-dimensional heat conduction in the layer renders the radiation-conduction interaction problem a complicated two-dimensional one. Further experimental and theoretical studies on the two-dimensional radiation-conduction interaction are needed.

## References


[1] Vliet, G. C. and Coston, R. M., "Thermal Energy Transport Parallel to the Laminations in Multilayer Insulation," *Advances in Cryogenic Engineering*, Vol. 13, 1968, pp. 671–679.

[2] Androulakis, J. G. and Kosson, R. M., "Effective Thermal Conductivity Parallel to the Laminations and Total Conductance for Combined Parallel and Normal Heat Flow in Multilayer Insulation," *Journal of Spacecraft and Rockets*, Vol. 6, No. 7, July 1969, pp. 841–845.

[3] Tien, C. L., Jagannathan, P. S., and Armaly, B. F., "Analysis of Lateral Conduction and Radiation Along Two Parallel Long Plates," *AIAA Journal*, Vol. 7, No. 9, Sept. 1969, pp. 1806–1808.

[4] Edwards, D. K. and Tobin, R. D., "Effect of Polarization on Radiant Heat Transfer Through Long Passages," *Journal of Heat Transfer*, Vol. 89C, 1967, pp. 132–138.

[5] Sparrow, E. M. and Cess, R. D., *Radiation Heat Transfer*, Brooks/Cole, Belmont, Calif., 1967.

[6] Cunnington, G. R. et al., "Performance of Multilayer Insulation Systems for Temperature to 700°K," CR-907, 1967, NASA.

[7] Cunnington, G. R., private communication, Lockheed Research Lab., Palo Alto, Calif., 1970.

[8] Tien, C. L. et al., "Thermal Conductivity of Thin Metallic Films and Wires at Cryogenic Temperatures," *Proceedings of Eighth Thermal Conductivity Conference*, Plenum Press, New York, 1969, pp. 13–20.

[9] Coston, R. M. and Vliet, G. C., "Thermal Energy Transport Characteristics Along the Laminations of Multilayer Insulations," *Thermophysics of Spacecraft and Planetary Bodies*, Academic Press, New York, 1968, pp. 909–923.

[10] Jagannathan, P. S., "Lateral Heat Transfer in Multilayer Insulation," Ph.D. thesis, Jan. 1971, Univ. of California.

[11] Pogson, J. T. and MacGregor, R. K., "A Method of Increasing the Lateral Thermal Resistance of Multilayer Insulation Blankets," AIAA Paper 70-15, New York, 1970.


# Performance of Disk-Gap-Band, Ringsail, and Cross Parachutes at Low Earth Altitudes


Harold N. Murrow* and Clinton V. Eckstrom*
*NASA Langley Research Center, Hampton, Va.*


RECENT work at the NASA Langley Research Center concerning the use of parachutes in a low-density environment was aimed at studying decelerator operation at supersonic velocities and low dynamic pressures corresponding to expected conditions during terminal descent for landing on the planet Mars.[1] In order to obtain quantitative data concerning performance differences of lightweight geometrically porous parachutes between low- and high-density operations, 11 low-altitude flight tests were conducted at the Joint Parachute Test Facility at El Centro, Calif. It was hoped that correlation of the resulting data could lead to high-altitude performance predictions by conducting easier and more economical low-altitude tests. The test dynamic pressure $q$ was adjusted upward for the low-altitude (high-density) tests in an attempt to obtain peak loadings similar to that experienced at high altitude. This Note discusses comparative high- and low-altitude performance characteristics of disk-gap-band (DGB), modified ringsail (RS), and cross parachute configurations which are shown in Fig. 1. The test payload configurations for both rocket-launched high-altitude tests and aircraft-dropped low-altitude tests were similar. Deployments for both test series were initiated by means of a mortar system,[2] whereby the parachute bridle, riser, and suspension lines deploy first, and a line stretch or snatch force occurs as the skirt portion of the canopy begins to leave the packing bag.

## Results

Load-time histories from the high- and low-altitude tests of the DGB parachute are compared in Fig. 2a. The low-altitude test deployment was initiated at 10,300 ft and a $q$ of 75 psf (a velocity of 300 fps), whereas the test at 140,000 ft was initiated at a $q$ of only 11.6 psf (2030 fps). Although the low-altitude deployment was initiated at the higher $q$, the opening load was less because of the much larger decrease in $q$ during the inflation sequence. For the high-altitude test,[3] $q$ decreased very little during the inflation process, and the maximum loading came very near the time of first full inflation, although the equilibrium canopy loading $W/C_DS$


Presented as Paper 70-1164 at the AIAA Aerodynamic Deceleration Systems Conference, Dayton, Ohio, September 14–16, 1970; submitted October 2, 1970; revision received December 16, 1970.



* Aerospace Technologist. Member AIAA.

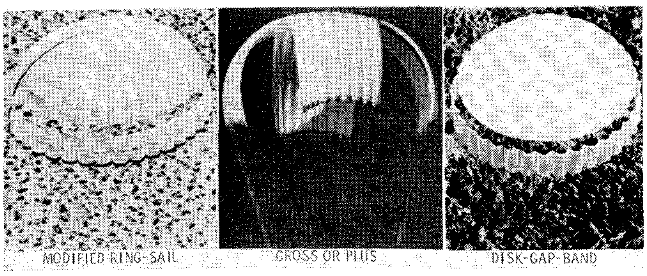


**Fig. 1 Photographs of test parachute configurations.**

was less than 0.45 psf. For both high- and low-altitude tests, the percentage of canopy inflation was determined from projected area obtained from the onboard camera film. For low-altitude tests, the maximum load is encountered early in the inflation process, primarily because the product of the frontal area $A$ (increasing with time) and $q$ (decreasing with time) is highest early in the opening sequence. Because $q$ changes so rapidly in the low-altitude tests, slight changes in the canopy inflation rate or process result in large and significant changes in the maximum opening load experienced; therefore, maximum loads are less repeatable. Note that first full inflation is much later in the low-altitude tests, and this is primarily a result of overinflation which occurs immediately after maximum loading.

Figure 2b compares results for a 30-ft-nominal-diameter modified ringsail parachute. The maximum opening load for the low-altitude test occurred nearer the time of full inflation than for the DGB parachute; however, for all low-altitude tests, the maximum load occurred prior to full steady canopy inflation. For the low-altitude test, $qA$ reached a maximum (maximum opening load) when the parachute canopy had achieved about 60% full inflation, even though $q$ decreased from 72 to about 15 psf during the inflation process. Since the maximum opening load encountered for this test was much greater than expected, another drop test of the same parachute was initiated at a lower deployment $q$. The opening load was reduced slightly, but this time the parachute was extensively damaged as it neared the full open condition. This emphasized the significance of the variation in opening loads that can be expected for low-altitude test conditions. A complete report of the high-altitude test is presented in Ref. 2.

For the cross parachute, three low-altitude tests were performed, and results from a low- and high-altitude test are compared in Fig. 2c. The low-altitude test results showed a considerable variation, although the highest loading is attributable mainly to the greater suspended weight for that test. In each low-altitude test, the maximum loading came well before full inflation. The $q$ at maximum loading ranged from 26 to 38 psf, with the lowest value of maximum opening load occurring at $q$ of 37 psf. From the estimated opening load history for the third test, where the total system weight was 600 lb, indications are that the load remained near 6000-lb for ~0.5 sec, indicating that the growth rate of $A$ was proportional to the decay rate of $q$ for an extended time interval. The load

**Table 1 Comparison of effective drag coefficient data**

| Test parachute | Altitude range, kft | $(C_{D,0})_{eff}$ |
|---|---|---|
| 40-ft disk-gap-band | 140 to 20 | 0.53[a] |
| | 8 to 0 | 0.55[a] |
| 30-ft modified ringsail | 113 to 77 | 0.52[a] |
| | 48 to 0 | 0.63[a] |
| 30-ft cross | 120 to 18 | 0.78[b] |
| | 8 to 0 | 0.70,[b] 0.72,[b] 0.76[b] |

[a] Based on total cloth area and geometric porosity.
[b] Based on total cloth area only.

oscillations shown for the high-altitude test[4] were attributed to the shape instability encountered with the cross parachute at supersonic test velocities. This "scissoring," ~4 cps, disappeared as the system decelerated to subsonic velocities.

For the high-altitude tests of the three parachute configurations, the effective drag-coefficient data, based on descent rate and system weight, were determined as the systems descended in the range from 140,000 ft to 20,000 ft altitude. For the low-altitude test, the $(C_{D,0})_{eff}$ data were obtained from about 8000 ft to sea level. Because of the significant difference in altitude range, the comparison of data, as shown in Table 1, was of interest. For the DGB and cross parachute, the high- and low-altitude results are closely comparable. However, for the ringsail parachute, there is a significant difference in $(C_{D,0})_{eff}$ at the lower altitude. This is at present unexplained, but it is to be noted that the "parachute handbook"[5] refers to significant variations in $(C_{D,0})_{eff}$ resulting from different descent rates for this particular canopy configuration. The descent rates used were 260–110 fps for the high-altitude flight tests and 31–26 fps for low-altitude tests.

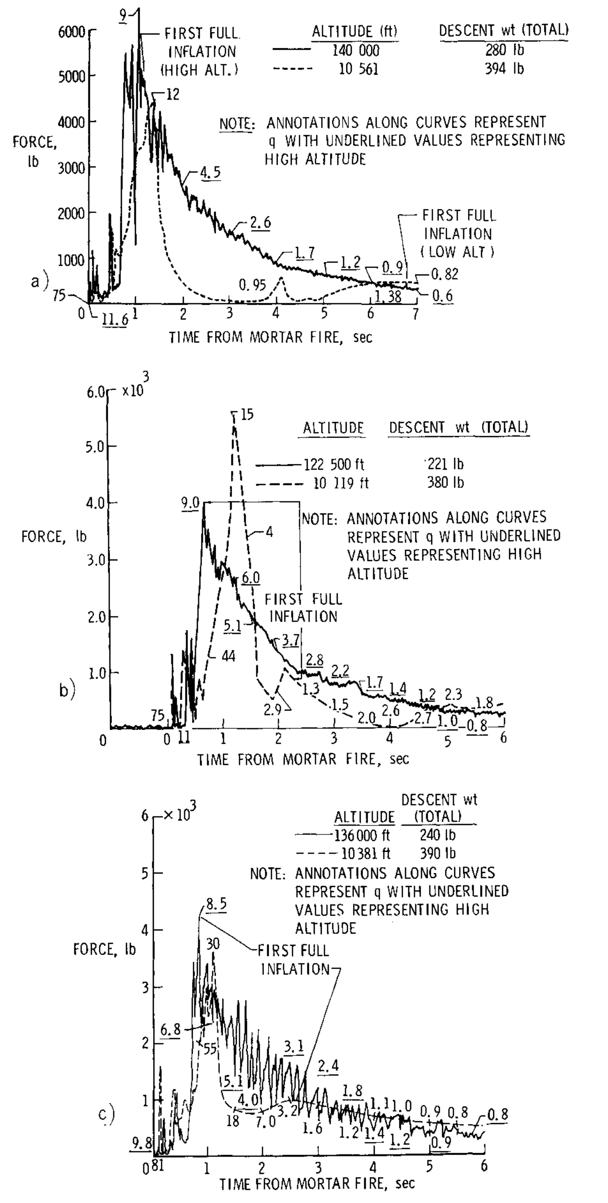


**Fig. 2 Load histories for high- and low-altitude deployments of a) 40-ft disk-gap-band, b) 30-ft modified ringsail, and c) 30-ft cross parachutes.**

**Table 2 Significant parameters applicable to low- and high-altitude tests**

| $W$,[a] lb | Parachute type | $D_0$, ft | Altitude, ft | $M$ | $q$, psf | $\Delta q/\Delta t$, psf/sec (avg.) | $m_a$,[b] lb |
|---|---|---|---|---|---|---|---|
| 280 | Disk-gap-band | 40.0 | 140,000 | 1.91 | 11.6 | 3.9[c] | 0.007 |
| 221 | Modified ringsail | 31.2 | 122,500 | 1.39 | 11.0 | 4.6 | 0.006 |
| 240 | Cross | 30.0 | 136,000 | 1.57 | 9.7 | 2.8 | 0.003 |
| 394 | Disk-gap-band | 40.0 | 10,600 | 0.35 | 73.9 | 54.0 | 70.0 |
| 380 | Modified ringsail | 31.2 | 10,100 | 0.34 | 76.9 | 55.0 | 33.0 |
| 390 | Cross | 30.0 | 10,400 | 0.28 | 80.9 | 49.0 | 30.0 |
| 394 | Cross | 30.0 | 10,600 | 0.27 | 75.4 | 48.0 | 30.0 |

[a] Total descent system weight.
[b] Apparent mass $m_a$ assumed equal to $\rho V/4$ ($V$ = projected-area-hemisphere volume = $2A^{3/2}/3(\pi)^{1/2}$.
[c] $\Delta q$ change in the interval between line stretch and peak load.

## Discussion

Table 2 compares the parameters considered to be significant in affecting parachute performance for the tests to be discussed in this paper, that is, $q$, Mach number $M$, altitude, and system weight.

Probably the most significant difference in deployment characteristics between high- and low-altitude tests observed by onboard camera film is the effect of the "apparent mass" $m_a$ at low altitude. For Table 2, $m_a$ is assumed to be equal to $\rho V/4$, where $\rho$ is the local air density and $V$ is the volume of a hemisphere with a diameter equal to the projected diameter (two-thirds nominal diameter) of the parachute. This $m_a$ is ~0.005 lb at high altitude and 30 to 70 lb at low altitude. (The weight of the parachute canopies was about 20 lb.) At low altitude, immediately after canopy inflation and rapid system deceleration, the canopy became significantly distorted, due to the effect of the mass of air in the wake not decelerating along with the flight system, which the authors refer to herein as an "apparent mass effect." This condition is sometimes called "over-inflation." The cross parachute was much less affected by this effect than the other two canopies.

The $M$'s for the low-altitude tests had to be subsonic to avoid prohibitive loadings for the test canopies. For high-altitude tests with deployments above $M = 2$, the canopies opened to full inflation and then exhibited a partial inflation and a corresponding lower average drag than that exhibited at lower velocities. The dynamic pressure change with time ($\Delta q/\Delta t$ in Table 2) during inflation was essentially an order of magnitude less at high altitude, as compared to low altitude (2.5-5 psf/sec vs 48-55 psf/sec). At high altitudes, peak loading corresponded to first full inflation, while at low altitude, peak loading occurred prior to full inflation. Thus, when deploying essentially the same system at different altitudes, a significant load-alleviating effect is seen with decreasing altitude due to the larger velocity decay during inflation and, thus, for a given parachute system, deployment without structural damage can be initiated at a higher $q$ at low altitude.

The test results presented have been from parachutes fabricated of cloth having a permeability range of 70 to 160 ft$^3$/min-ft$^2$ at a differential pressure of 0.5 in. of water. The effects of a wider range of cloth permeability (effective porosity) on opening and stability characteristics of parachutes over large altitude differences are, as yet, unknown. Some research on this effect appears warranted.

These low- and high-altitude data have been correlated nicely by Greene[6] to show that the opening distance of a parachute varies with $M$. Further analyses such as these may make it possible to conduct low-altitude drop tests and use the results to predict performance at high altitude. At the present time, it appears that the performance differences over large altitude increments are not sufficiently predictable to use this technique to advantage.

## References

[1] Murrow, H. N. and McFall, J. C., "Summary of Experimental Results Obtained From the NASA Planetary Entry Parachute Program," *Proceedings of FTC-TR-69-11*, Air Force Flight Test Center, 1969; also *Journal of Spacecraft and Rockets*, Vol. 6, No. 5, May 1969, pp. 621–623.

[2] Preisser, J. S., Eckstrom, C. V., and Murrow, H. N., "Flight Test of a 31.2-Foot-Diameter Modified Ringsail Parachute Deployed at a Mach Number of 1.39 and a Dynamic Pressure of 11.0 Pounds Per Square Foot," TM X-1414, Aug. 1967, NASA.

[3] Preisser, J. S. and Eckstrom, C. V., "Flight Test of a 40-Foot-Nominal-Diameter Disk-Gap-Band Parachute Deployed at a Mach Number of 1.91 and a Dynamic Pressure of 11.6 Pounds Per Square Foot," TM X-1575, May 1968, NASA.

[4] Preisser, J. S. and Eckstrom, C. V., "Flight Test of a 30-Foot-Nominal-Diameter Cross Parachute Deployed at a Mach Number of 1.57 and a Dynamic Pressure of 9.7 Pounds Per Square Foot," TM X-1542, April 1968, NASA.

[5] "Performance of and Design Criteria for Deployable Aerodynamic Decelerators," ASD-TR-61-579, Dec. 1963, U.S. Air Force.

[6] Greene, G. C., "Opening Distance of a Parachute," *Journal of Spacecraft and Rockets*, Vol. 7, No. 1, Jan. 1970, pp. 98–100.

# A 30-cm Mercury Ion Thruster Module

H. J. KING* AND R. L. POESCHEL†
*Hughes Research Laboratories, Malibu, Calif.*

In an earlier paper,[1] the scaling and development of a SERT II thruster design to 30-cm diam was presented. This Note describes the optimization procedures and performance characteristics of the thruster system which has evolved during the ensuing period. A principal task was the selection of an ion optical system for operation at a specific impulse ($I_{sp}$) of 2750 sec. Several designs of conventional two-grid systems and single, dielectric-coated grid systems were evaluated experimentally, and a single grid system (having apertures of 0.2-cm diam on 0.25-cm center-to-center spacing in hexagonal array) was the best of the systems tested at that time. The next task was to optimize the thruster discharge chamber for operation at the 27 mlb thrust level.

The optimization effort drew heavily on the results of Bechtel[2] and communications with other NASA LeRC staff members. On the basis of this information, the only parameters which required modification were magnetic field strength and baffle size. Included in the optimization effort was the integration of a hollow cathode plasma bridge neutralizer, as well as several other components necessary to complete the thruster module, including a more durable thruster cathode, propellant electrical isolators and efficient propellant vaporizers. The complete thruster module was tested for 500 hr. All components performed well. With the exception of the dielectric grid all component lifetimes can be extrapolated to more than 10,000 hr. Although several reasons for the failure of the dielectric optics have been postulated (i.e., back-sputtered material from the beam collector, inhomo-

Presented as Paper 70-1099 at the AIAA 8th Electric Propulsion Conference, Stanford, Calif., August 31–September 2, 1970; submitted October 23, 1970; revision received December 18, 1970. Supported in part by NASA-Lewis Research Center.

* Head, Propulsion Technology Section. Associate Fellow AIAA.

† Senior Staff Engineer. Member AIAA.